

Stereocilia Bundle Imaging with Nanoscale Resolution in Live Mammalian Auditory Hair Cells

Carolina Galeano-Naranjo^{1,2}, A. Catalina Veléz-Ortega¹, Gregory I Frolenkov¹

¹ Department of Physiology, College of Medicine, University of Kentucky ² Universidad Nacional de Colombia

Corresponding Authors

A. Catalina Veléz-Ortega

catavelezo@uky.edu

Gregory I Frolenkov

gregory.frolenkov@uky.edu

Citation

Galeano-Naranjo, C., Veléz-Ortega, A.C., Frolenkov, G.I. Stereocilia Bundle Imaging with Nanoscale Resolution in Live Mammalian Auditory Hair Cells. *J. Vis. Exp.* (), e62104, doi:10.3791/62104 (2021).

Date Published

January 11, 2021

DOI

10.3791/62104

URL

jove.com/t/62104

Abstract

Inner ear hair cells detect sound-induced displacements and transduce these stimuli into electrical signals in a hair bundle that consists of stereocilia that are arranged in rows of increasing height. When stereocilia are deflected, they tug on tiny (~5 nm in diameter) extracellular tip links interconnecting stereocilia, which convey forces to the mechanosensitive transduction channels. Although mechanotransduction has been studied in live hair cells for decades, the functionally important ultrastructural details of the mechanotransduction machinery at the tips of stereocilia (such as tip link dynamics or transduction-dependent stereocilia remodeling) can still be studied only in dead cells with electron microscopy. Theoretically, scanning probe techniques, such as atomic force microscopy, have enough resolution to visualize the surface of stereocilia. However, independent of imaging mode, even the slightest contact of the atomic force microscopy probe with the stereocilia bundle usually damages the bundle. Here we present a detailed protocol for the hopping probe ion conductance microscopy (HPICM) imaging of live rodent auditory hair cells. This non-contact scanning probe technique allows time lapse imaging of the surface of live cells with a complex topography, like hair cells, with a single nanometers resolution and without making physical contact with the sample. The HPICM uses an electrical current passing through the glass nanopipette to detect the cell surface in close vicinity to the pipette, while a 3D-positioning piezoelectric system scans the surface and generates its image. With HPICM, we were able to image stereocilia bundles and the links interconnecting stereocilia in live auditory hair cells for several hours without noticeable damage. We anticipate that the use of HPICM will allow direct exploration of ultrastructural changes in the stereocilia of live hair cells for better understanding of their function.

Introduction

Despite the fact that stereocilia bundles in the auditory hair cells are big enough to be visualized by optical microscopy and deflected in live cells in a patch clamp experiment, the essential structural components of the transduction machinery such as tip links could be imaged only with the electron microscopy in dead cells. In the mammalian auditory hair cells, the transduction machinery is located at the lower ends of the tip links, i.e., at the tips of the shorter row stereocilia¹ and regulated locally through the signaling at the tips of stereocilia^{2,3}. Yet, label-free imaging of the surface structures at this location in live hair cells is not possible due to the small sizes of stereocilia.

The mammalian cochlea has two types of auditory sensory cells: inner and outer hair cells. In the inner hair cells, stereocilia are longer and thicker compared to those in the outer hair cells⁴. The first and second row of stereocilia have a diameter of 300-500 nm in mouse or rat inner hair cells. Due to the diffraction of light, the maximum resolution achievable with a label-free optical microscopy is approximately 200 nm. Hence, visualization of individual stereocilia within first and second rows of the inner hair cell bundle is relatively easily with optical microscopy. In contrast, shorter row stereocilia in the inner hair cells and all stereocilia of the outer hair cells have diameters around 100-200 nm and cannot be visualized with optical microscopy⁵. Despite recent progress in super-resolution imaging, this fundamental limitation persists in any optical label-free imaging. All current commercially available super-resolution techniques do require some sort of fluorescent molecules⁶, which limits their applications. In addition to limitations due to the need for specific fluorescently tagged molecules, exposure to intense light irradiation has been shown to induce cellular damage and might influence

cellular processes, which is a great disadvantage when studying live cells⁷.

Our current knowledge of the ultrastructural details of hair cell stereocilia bundles has been obtained mostly with various electron microscopy (EM) techniques, such as scanning electron microscopy (SEM), transmission electron microscopy (TEM), freeze-fracture EM, and recently with 3D techniques such as serial sectioning with focused ion beam or cryo-EM tomography^{8,9,10,11,12,13,14,15,16}. Unfortunately, all these EM techniques require chemical or cryofixation of the sample. Depending on the time scale of the phenomena, this requirement makes a study of the dynamic processes at the tips of stereocilia either impossible or very labor intensive.

Limited efforts have been made to image hair bundles of live hair cells with atomic force microscopy (AFM)^{17,18}. Since AFM operates in physiological solutions, it could, in theory, visualize dynamic changes in the stereocilia bundles of live hair cells over time. The problem lies in the principles of high-resolution AFM, which implies certain physical contact between the AFM probe and the sample, even in the least damaging "tapping" mode¹⁹. When the AFM probe encounters a stereocilium, it usually crashes against it, damaging the structure of the hair bundle. As a result, this technique is not suitable for visualizing live, or even fixed, hair cells bundles^{17,18}. The problem may be partially alleviated by using a large ball-shaped AFM probe that imposes only hydrodynamic forces to the surface of the sample²⁰. However, even though such a probe is ideally suited to test mechanical properties of the sample²¹, it provides only a sub-micrometer resolution when imaging the organ of Corti²² and still applies to the sample a force that may be substantial for the highly sensitive stereocilia bundles.

Scanning ion conductance microscopy (SICM) is a version of scanning probe microscopy that uses a glass pipette probe filled with a conductive solution²³. SICM detects the surface when the pipette approaches the cell and the electric current through the pipette decreases. Since this is happening well before touching the cell, the SICM is ideally suited for non-contact imaging of live cells in physiological solution²⁴. The best resolution of SICM is on the order of single nanometers, which allows resolving individual protein complexes at the plasma membrane of a living cell²⁵. However, similar to other scanning probe techniques, SICM is able to image only relatively flat surfaces. We overcame this limitation by inventing hopping probe ion conductance microscope (HPICM)²⁶, in which the nanopipette approaches the sample at each imaging point (**Figure 1A**). Using HPICM, we were able to image stereocilia bundles in live auditory hair cells with nanoscale resolution²⁷.

Another fundamental advantage of this technique is that HPICM is not only an imaging tool. In contrast to other scanning probe techniques, the HPICM/SICM probe is an electrode widely used in cell physiology for electrical recordings and local delivery of various stimuli. Ion channel activity does not usually interfere with HPICM imaging, because the total current through the HPICM probe is several orders of magnitude larger than the extracellular current generated by the largest ion channels²⁵. However, HPICM allows precise positioning of the nanopipette over a structure of interest and subsequent single-channel patch-clamp recording from this structure²⁸. This is how we obtained the first preliminary recordings of single channel activity at the tips of the outer hair cell stereocilia²⁹. It is worth mentioning that even a large current through the nanopipette cannot produce significant changes of the potential across the plasma membrane due to enormous electrical shunt of

the extracellular medium. However, individual ion channels can be activated mechanically by flow of liquid through the nanopipette³⁰ or chemically by local application of an agonist³¹.

In HPICM, the image is generated when a nanopipette sequentially approaches the sample at one point, retracts, and then moves in lateral direction to repeat the approach (**Figure 1A**). A patch clamp amplifier constantly applies voltage to an AgCl wire in the pipette (**Figure 1B**) to generate a current of ~1 nA in the bath solution. The value of this current when the pipette is away from the surface of the cell is determined as a reference current (I_{ref} , **Figure 1C**). Then, the pipette moves in the Z axis to approach the sample until the current is reduced by an amount predefined by the user (setpoint), usually 0.2%-1% of the I_{ref} (**Figure 1C**, top trace). The system then saves Z value at this moment as the height of the sample, together with X and Y coordinates of this imaging point. Then, the pipette is retracted away from the surface (**Figure 1C**, bottom trace) at a speed defined by the user, usually 70–90 nm/ms. After retraction, the pipette (or, in our case, the sample - see **Figure 1B**) is moved laterally to the next imaging point, a new reference current value is obtained, and the pipette once again approaches the sample, repeating the process. The X-Y movement of the pipette is preferred in an upright microscope setup that is typically used for recordings of the hair cell mechanotransduction currents. In this setting, the HPICM probe approaches the hair cell bundles not from the top but at an angle³². However, the best resolution of HPICM imaging is achieved in an inverted microscope setup (**Figure 1A,B**), where the movement of the sample in X-Y directions is de-coupled from Z-movement of the nanopipette, thereby eliminating potential mechanical artefacts.

Using HPICM, we obtained topographic images of mouse and rat inner and outer hair cell stereocilia bundles, and even visualized the links between the stereocilia that are about 5 nm in diameter^{26,27}. The success of hair cell bundle imaging with this technique relies on several factors. First, the noise (variance) of the nanopipette current should be as small as possible to allow the lowest possible setpoint for HPICM imaging. A low setpoint allows HPICM probe to “sense” stereocilia surface at a larger distance and at any angle to the probe approach and, surprisingly, improves X-Y resolution of HPICM imaging (see **Discussion**). Second, the vibrations and drifts in the system should be decreased to less than 10 nm, since they contribute directly to the imaging artefacts. Finally, even though the HPICM probe and the specimen stage are moved in Z and X-Y axes by the calibrated feedback-controlled piezo actuators that have an accuracy of a single nanometer or better, the diameter of the nanopipette tip determines the spread of the current (sensing volume) and hence the resolution (**Figure 1A**). Therefore, before imaging live hair cells, it is vital to pull the adequate pipettes, reach the desired resolution with calibration samples, and achieve low noise in the recording system.

For at least a couple of decades, the SICM technique has not been commercially available and it has been developing by only few labs in the world with the leading lab of Prof. Korchev in the Imperial College (UK). Recently, several SICM systems became commercially available (see **Table of Materials**), all of which are based on the original HPICM principles. However, imaging stereocilia bundles in the hair cells requires several custom modifications that are technically challenging (or even impossible) in the closed “ready-to-go” systems. Therefore, some component integration is needed. Since HPICM setup represents a patch clamp rig with more stringent

vibration and drift requirements and a piezo-driven movement of the HPICM probe and the sample (**Figure 1D**), this integration is relatively easy for any researcher, who is proficient in patch clamping. However, a scientist without proper background would definitely need some training in electrophysiology first. Despite remaining challenges such as increasing the speed of imaging (see **Discussion**), we have been able to image stereocilia bundles in live hair cells with nanoscale resolution without damaging them.

This paper presents a detailed protocol to perform successful HPICM imaging of the live auditory hair cell bundles in young postnatal rat or mouse cochlear explants using our custom system. The integrated components are listed in the **Table of Materials**. The paper also describes common problems that can be encountered and how to troubleshoot them.

Protocol

The study was performed in accordance with the recommendations in the Guide for the Care and Use of Laboratory Animals of the National Institutes of Health. All animal procedures were approved by the Institutional Animal Care and Use Committee (IACUC) at the University of Kentucky (protocol 00903M2005).

~~The study was performed in accordance with the recommendations in the Guide for the Care and Use of Laboratory Animals of the National Institutes of Health. All animal procedures were approved by the Institutional Animal Care and Use Committee (IACUC) at the University of Kentucky (protocol 00903M2005).~~

1. Manufacturing and testing the nanopipettes

1. Create a program in the micropipette puller to obtain pipettes with a resistance between 200 and 400

MΩ, which corresponds to inner tip diameters of approximately 50-70 nm. The parameters will depend on the micropipette puller. To obtain short pipettes with non-flexible fine tips, check in the operational manual of the puller.

2. Use borosilicate glass capillaries with outer/inner diameters of 1/0.58 mm and an inner filament to facilitate filling. The length of the pipette is crucial because it determines the frequency of the lateral mechanical resonance of the pipette. The longer is the pipette, the lower is the resonant frequency and the harder is to avoid this resonance.

NOTE: The user should try to manufacture the shortest pipette the holder can accept. The length of nanopipettes in this experiment is usually 15-25 mm (**Figure 2A**).

3. Fill the nanopipette up to its middle point (**Figure 2A**) with a bath solution, either Leibovitz's L-15 or with Hank's Balanced Salt Solution (HBSS) supplemented with 20 mM D-glucose (to adjust osmolarity). To avoid potential artefacts, use the same solution that will be used in the bath for recordings.
4. Using an optical microscope with a magnification of 10x, check for any bubbles at the tip of the pipette (**Figure 2B**). The bubbles would prevent the current flow. It is harder to remove bubbles in the pipettes that have been pulled several hours before the experiment. Therefore, it is recommended to pull new pipettes with every experiment.
5. Once the pipette is free of bubbles, mount it in the HPICM pipette holder (**Figure 2C**).
6. Place the sample (tissue or calibration standard) on the custom-built chamber and add 4 mL of the above-mentioned bath solution.

7. Place a custom-built chamber on the HPICM stage and introduce the ground electrode in the solution.
8. Make sure that the voltage being applied to the pipette by the patch clamp amplifier is zero.
9. Move the pipette in Z until it touches the liquid.
10. Set the amplifier offset to zero and then add +100 mV to check the pipette current.

11. Calculate the resistance and the diameter of the pipette, based on Ohm's law:

$$R = V/I$$

where R is the resistance (MΩ), V is the voltage applied to the nanopipette (mV) and I is the current flowing through the nanopipette (nA).

1. Calculate the inner diameter of the pipette as described elsewhere according to the following formula¹²:

$$ID_{Tip} = 1000/\sqrt{R}$$

NOTE: The ideal resistance value is between 200 and 400 MΩ. Pipettes with a resistance higher than 400 MΩ might lead to an unstable current due to their small size (< 50 nm inner diameter). On the contrary, pipettes with resistances smaller than 200 MΩ are too large (> 70 nm inner diameter) and would not resolve small features. It is recommended to start imaging with the pipettes of 200 MΩ resistance, as they are easier to manufacture and tend to provide less electrical noise.

2. Minimizing sample drifts and vibrations

NOTE: To decrease the mechanical noise in the system during imaging, mount the samples on the custom-built chambers that utilize thick glass slides (~1.2 mm):

1. Remove the glass portion off a 50 mm glass-bottom dish, leaving the plastic walls intact.
2. Glue the plastic portion of the cell culture dish on top of the thick glass slide with silicon glue.
3. Mount the calibration sample in the middle of the chamber (on top of the glass slide) using either silicon glue or thin double-sided tape.
4. Firmly secure the chamber onto the HPICM stage using double-sided tape.
5. During imaging, close the Faraday cage and cover it with a blanket to minimize electrical interference and thermal drift, correspondingly.
2. Add 4 mL of HBSS to the chamber to cover the calibration sample. Then, secure the chamber to the XY stage of the HPICM setup using double-sided tape.
3. Clamp the magnetic holder of the ground electrode to the stage near the chamber and immerse the electrode into the bath solution (**Figure 1B**).
4. Mount the nanopipette into the holder, immerse it into the bath solution, and set its current to ~1 nA following the steps described in Section 1.
5. Position the nanopipette approximately above the center of the calibration standard using a course patch-clamp manipulator. Visual inspection is usually enough for this positioning, since the area covered by silicon dioxide structures is relatively large (1 x 1 mm). In contrast to the organ of Corti explants (see below), calibration standard is non-transparent and, therefore, a more precise positioning guided by optical imaging is not possible for this sample.

3. Testing the resolution with AFM calibration standards

NOTE: It is strongly recommended to image AFM standards (see **Table of Materials**) before imaging live cells in order to troubleshoot the system and test its resolution in the X-Z-Y axes. The calibration standards have silicon dioxide pillars and holes of different shapes but fixed heights/depths (i.e., 20 or 100 nm) on a 5 x 5 mm silicon chip. Starting with the 100 nm calibration standard is recommended, to guarantee that the Z resolution is below 100 nm. After achieving a successful high-resolution image of the pillars or holes in this calibration sample (**Figure 3A**), move to the 20 nm standard. If the imaging of the latter standard is successful (**Figure 3B**), the resolution in the Z axis is guaranteed to be below 20 nm and appropriate for the imaging of the hair cell stereocilia bundles¹². The following steps are used to image both calibration standards.

1. Attach the calibration standard to the chamber with silicon glue.
6. Increase the setpoint while monitoring the signal from the sensor of the Z piezo actuator on an oscilloscope in a real time. After establishing a stable repeatable Z approach cycle (as in **Figure 1C**, bottom), decrease the setpoint to the value that is just above the point of instability. This procedure would ensure the optimal setpoint for this particular nanopipette.
7. Move the pipette down at a speed of ~5 $\mu\text{m/s}$ with a patch clamp micromanipulator until it reaches the sample. At this moment, the bottom level of the real-time Z positioning signal (**Figure 1C**) will increase, indicating that the nanopipette is withdrawn due to "sensing" the sample surface. Any further movement of the nanopipette will result in further positive shift of Z-positioning signal.

NOTE: Be careful not to exceed the upper limit of Z piezo actuator movement.

8. Start imaging at low resolution (see **Table 1**). Due to uneven mounting of the AFM standard, the highest point of the area of interest may be unknown. Therefore, set the amplitude of pipette retraction (hop amplitude) to at least 200-500 nm.
 1. Once the highest point of the sample in the imaging area is identified, decrease the hop amplitude. A smaller hop amplitude allows faster scanning, which is preferred for high resolution imaging due to diminished effects of the drifts and decreased vibration.
9. Before moving the pipette to a new X-Y location, retract it about 200 μm in the Z axis to prevent any undesired collisions with the sample.

NOTE: In cases when the nanopipette is not aligned with the center of the calibration standard, it is possible that the scanning starts just off the area of surface features.
10. After the area of interest is found, start imaging at a higher resolution (see **Table 1**).

4. Making custom-built chambers to secure the cochlear explants

NOTE: Mount the cochlear explants in the chambers with custom-built clamping systems that utilize either flexible glass pipettes (step 4.1) (**Figure 4A**) or dental floss (step 4.2) (**Figure 4B**). The glass pipette chamber could be sterilized and used for the cultured organs of Corti, while dental floss chamber provides a more secure holding of the sample and a control over stereocilia bundle orientation during mounting. These custom-built chambers need to be prepared

in advance, but they can be cleaned and re-used in several imaging sessions.

1. Make a chamber using flexible glass pipettes
 1. Pull two thin and flexible glass fibers from glass capillaries using a pipette puller. Our pulled glass fibers typically measure 1 to 2 cm in length and are fairly flexible.
 2. Place a small drop of the silicone elastomer on top of a glass coverslip. Use coverslips of 2 cm in diameter.
 3. Place the ends of two glass fibers on the silicone drop and arrange the fibers to have a small degree of separation between them (**Figure 4A**).
 4. Place the coverslip on a hot plate to quickly cure the elastomer (1 to 3 min).
 5. Glue the coverslip onto the glass bottom of the chamber described in Section 2 using a small amount (1-3 μL) of silicone elastomer and allowing it to cure overnight.
2. Making a chamber using dental floss:
 1. Remove the glass portion of a 50 mm glass-bottom dish, leaving the plastic walls intact. Then glue the plastic portion of the cell culture dish on top of a 1.2 mm thick glass slide with silicon glue.
 2. Mount one plastic coverslip (6.5 x 6.5 mm) with the same glue to the center of the chamber. Then repeat the process with another coverslip on top of the previous one.
 3. Mount two small tungsten or gold-plated wires (12 mm of length and ~ 0.5 mm in diameter) with silicon glue, each one at opposite sides of the cover slides.

Glue them far enough (> 10-15 mm) from the cover slides (**Figure 4B**).

4. Separate two dental floss strands and place them on top of the cover slides and secure them to the wires by making a knot. Leave a small gap between both strands (**Figure 4B**, short arrows).
3. Clean the chambers after every use
 1. Gently remove the tissue from the chamber using fine tweezers and lightly scrape any tissue residues left behind.
 2. Rinse the chamber first with 70% ethanol and then with distilled water.
 3. Repeat the rinse cycle if needed.
 4. Place the chamber upside down on a filter paper to let it dry until next experiment. The chambers do not need to be sterilized, unless culturing of the organ of Corti is planned after the imaging.

5. Dissecting the rodent organ of Corti

1. Perform dissection of the young postnatal cochlear explants as described in detail elsewhere¹³.
2. For HPICM imaging, dissect the organ of Corti from mice between postnatal days 3 and 6 (P3-6), and from rats between postnatal days 3 and 8 (P3-8).

NOTE: Older hair cells are more susceptible to the damage during dissection and, therefore, cannot be used for hours-long time lapse HPICM imaging.
3. Do not forget to remove the tectorial membrane before HPICM imaging.
4. Immediately after dissection, secure the tissue in one of the chambers described in Section 4, either placing it under the flexible glass pipettes or under the two dental

floss strands (**Figure 4**). Pre-fill these chambers with 4 mL of the room temperature bath solution (to minimize bubble formation).

6. Imaging of the auditory hair cells

1. Mount the chamber with a freshly isolated organ of Corti on the X-Y piezo stage using double-sided tape and make sure that it is firmly secured to minimize chamber drift in X and Y axes (**Figure 1B**).
2. Follow steps in Section 1 to place a new nanopipette and check for the correct pipette resistance.
3. Using patch clamp micromanipulator, position nanopipette over the hair cell region, while observing the organ of Corti explant in an inverted microscope.
4. Check if the system is stable with a setpoint of 0.5% or lower by recording the real-time current and Z positioning signal on the oscilloscope (as in **Figure 1C**). If Z signal is not stable, try to decrease the cutoff frequency of the low-pass filter of the patch clamp amplifier. However, it cannot be lower than the response time of Z piezo actuator (to avoid pipette collision with the sample due to delayed current readings).

NOTE: In practice, 5 kHz setting of this filter is found to be optimal. It is better to replace the nanopipette, if Z-signal is still unstable.
5. Once ~~a stable~~ a stable recording is achieved, determine the optimal setpoint and approach the sample with HPICM pipette as described in the steps 3.6-3.7 above.
6. First, perform low resolution imaging (see **Table 1**), using a hop amplitude of at least 6 to 8 μm . To image tall structures such as the hair cell stereocilia bundles, make sure that the hop amplitude is enough to avoid collision with these structures.

NOTE: If the hop amplitude is not enough, the pipette will not be able to jump over a stereocilium and there will be an imminent collision. The collision of the HPICM probe with a stereocilium may damage the hair bundle. Therefore, in cases when the height of the stereocilia bundle is uncertain, use a bigger hop amplitude.

7. Get familiar with the topography of the organ of Corti by first performing and/or studying images obtained with scanning electron microscopy (**Figure 5**).

NOTE: If the HPICM image is uniform with the heights smaller than 1 μm in every imaging point, the pipette is likely scanning the glass bottom and not the tissue. Alternatively, the pipette may "land" on a different region of the cochlear explant, away from the hair cells.

8. If the pipette needs to be moved to a new X-Y location, retract it about 500 nm to avoid collisions with any tall features within the tissue. Repeat low-resolution HPICM imaging until the region of interest with the hair cells is found.

9. After the region of interest is found, start imaging at a higher resolution (see **Table 1**). Try to spend less than 15 min when imaging a whole hair bundle.

NOTE: The hair cell bundles in the live tissue are not still but may change their orientation, for example, due to shape changes in the underlying supporting cells. Therefore, the images may exhibit movement artefacts if the image acquisition is too slow.

10. Once again, determine the tallest features in the low-resolution images before the decreasing the hop amplitude for high-resolution imaging. For a region of interest covering entire hair cell bundle, reduce the hop amplitude to 4-5 μm , while for a relatively small and "flat" region within the bundle (e.g., 2 x 2 μm) reduce the hop

amplitude even further, down to a less than 1 μm , thereby increasing the speed and resolution of imaging.

7. Image processing

NOTE: Imaging artefacts are common in HPICM imaging. Some of them can be corrected by image acquisition parameters, while others require post-processing either with a specialized SICM viewer or with more general data-processing programs like ImageJ or MatLab. Here we describe the most common artefacts and how we fix them with SICM viewer.

1. Perform slope correction

NOTE: It is not obvious for a beginner, but human eye cannot resolve sub-micrometer size features at the surface of a cell, if the imaging area has an overall slope of equal or larger size (**Figure 3A,B**, left). Therefore, it is necessary to determine the average slope of an imaged area (by fitting HPICM 3D image data to a single plane) and subtract it from the HPICM image (**Figure 3A,B**, middle).

1. Click **Open** to open an image with SICM viewer.
2. Select the **Image Correction** tab.
3. Select the **Correct Slope** tab.
4. Press the **Correct Slope** button for an automated slope correction.

2. Perform line alignment

NOTE: As mentioned before, mechanical and/or thermal drifts as well as cell movement artefacts represent a significant problem in HPICM imaging. A small drift with a speed of less than a micrometer per minute is usually not noticeable in a regular patch clamp setup. Yet, it could produce artefacts of several tens of nanometers in HPICM imaging, which is significantly larger than the

resolution of HPICM. Therefore, it is not uncommon to encounter sudden jumps in Z axis between two neighboring HPICM scan lines during imaging. This could be corrected by analyzing differences between starting (and/or ending) Z-values in these neighboring scan lines.

1. Click **Open** to open an image with SICM viewer.
2. Select the **Image Correction** tab.
3. Select the **Correct Slope** tab.
4. Choose the width of lines to be aligned. Press on the button **ButtonDestripeLineFit** for an automated line alignment correction.

3. Perform noise reduction

NOTE: While obtaining images with HPICM, small fluctuations in the nanopipette current can lead to the nanopipette stopping far from the surface of the sample, especially with low setpoints. It results in the appearance of small white dots in the image. In order to correct this imaging artefact, it is necessary to identify the imaging points with the Z-value significantly larger than that of the neighbors and replace this value with an average of the neighbors. This is be done by an adjustable median filter.

1. Click **Open** to open an image with SICM viewer.
2. Select the **Image Processing** tab.
3. Select the **Noise reduction** tab.
4. Set the **Threshold filter** (μm) for the pixels to be removed.

Representative Results

The protocol presented in this paper can be used to visualize any live cells with complex topography. Following these

steps, we routinely obtain images of live rat auditory hair cell bundles (**Figure 6B,D**). In spite of having lower X-Y resolution when compared to SEM images, our HPICM images can successfully resolve the different rows of stereocilia, the shape of the stereocilia tips, and even the small links (~ 5 nm in diameter) connecting adjacent stereocilia (**Figure 6F**). In addition, HPICM images have information in 3D that SEM images lack. Given the non-contact nature of this type of imaging technique, we were also able to perform continuous time-lapse HPICM imaging of the same hair cell bundle for several hours (i.e., 5-6 h regularly) without damaging the bundle cohesiveness (**Figure 7**). Thus, HPICM exhibits a great potential for the study of dynamic structural changes of the hair cell bundles over time.

Although we provide several ranges for pipette size, current setpoint, low- and high-resolution parameters, and hop amplitudes, each user might need to slightly optimize their settings to obtain successful HPICM images of live hair cell bundles. Smaller setpoints produce better quality images. However, with a very low setpoint, the system might interpret small fluctuations in the current as encountering the cell surface and this will lead to the "white dot" noise in the image (**Figure 8A**). Similarly, large hop amplitudes might increase the lateral resonance of the pipette and also produce noisy pixels (**Figure 8B**). In contrast, if the hop amplitude is too small or the setpoint is too high, the nanopipette might collide with the sample and lead to imaging artefacts or even damage the hair bundle (**Figure 8C,D**). We recommend performing the imaging at lower resolution while tweaking all these parameters to minimize damage to the sample or to the nanopipette.

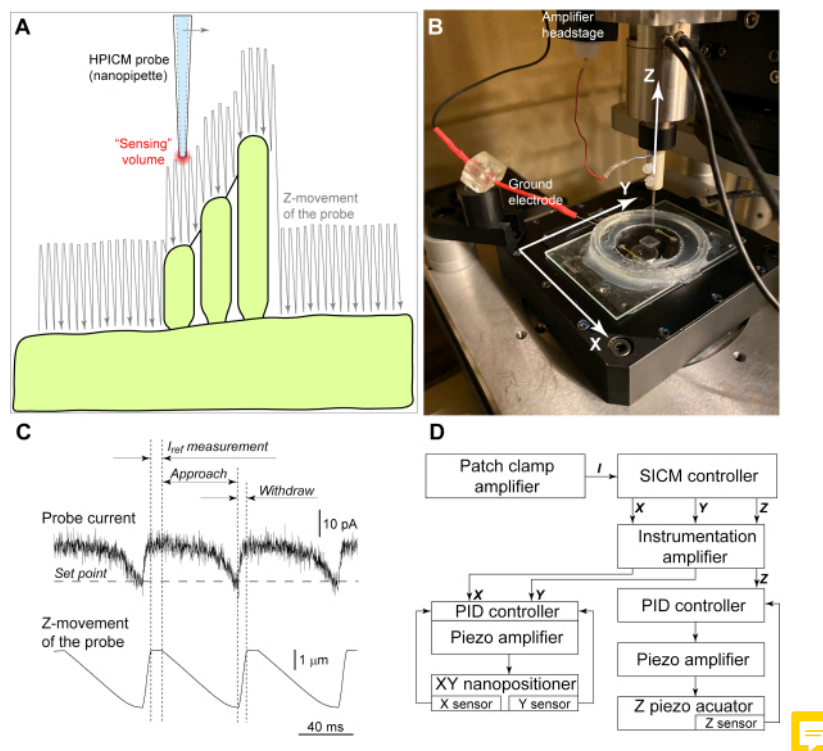


Figure 1: Principles of hopping probe ion conductance microscopy (HPICM). (A) An electric current passing through the nanopipette generates a "sensing volume" at the tip of the pipette. To image complex structures like the hair cell stereocilia bundles, the pipette approaches toward the cell surface from above and retracts after detecting the surface. After a lateral move at each step, the pipette continues to "hop" above the sample generating the image of the cell. Notice that the hop amplitude must be sufficient for the pipette to "climb" to a stereocilium. Illustrated hop amplitude would work for left-to-right scanning (from smallest to a tallest stereocilium, indicated by an arrow). However, it is too small for right-to-left scanning when the pipette meets the tallest stereocilium first. (B) Experimental setup. A custom-made chamber with the organ of Corti explant is mounted on a XY nanostaging stage with an aperture for optical microscopy observation. The nanopipette is moved by a separate ultra-fast Z piezo actuator. To position the nanopipette over the region of interest, Z actuator is mounted on a conventional micromanipulator (not shown) together with the patch clamp *amplifier headstage*. *Ground electrode* is mounted on a magnetic holder and inserted into the bath. (C) Representative recordings of the pipette current (*top trace*) and Z position of the pipette (*bottom trace*) during imaging. When the pipette is away from the cell surface, the reference value of the current passing through the pipette is determined (I_{ref}). Then, the pipette is moved toward the sample (*approach*). When the "sensing volume" meets the cell surface, the pipette current starts decreasing. The command for withdrawal is issued when the current decrease reaches a setpoint, which is typically 0.2% - 1% of I_{ref} . (D) Schematics of the equipment that need to be added to a conventional patch clamp setup for HPICM imaging. A dedicated **patch clamp amplifier** records the nanopipette current (I) that is used by SICM controller in HPICM mode to generate command signals

to X, Y, and Z axes. **Instrumentation amplifier** provides offset, scaling, and low pass filtering to these signals, if needed. Unfortunately, X/Y/Z signals from the controller cannot be applied directly to the piezo actuators due to large errors caused by hysteresis and creeping that are inherent to piezo ceramic. Therefore, each *piezo actuator (translation stage)* has a built-in motion sensor that sends feedback signal to the proportional-integral-derivative (PID) controller that pre-shapes the command signal to correct for these errors. Note that relatively slow X and Y axes could use *PID controllers* that are built in the *piezo amplifier*, while a faster Z axis requires a dedicated fast *PID controller*. [Please click here to view a larger version of this figure.](#)

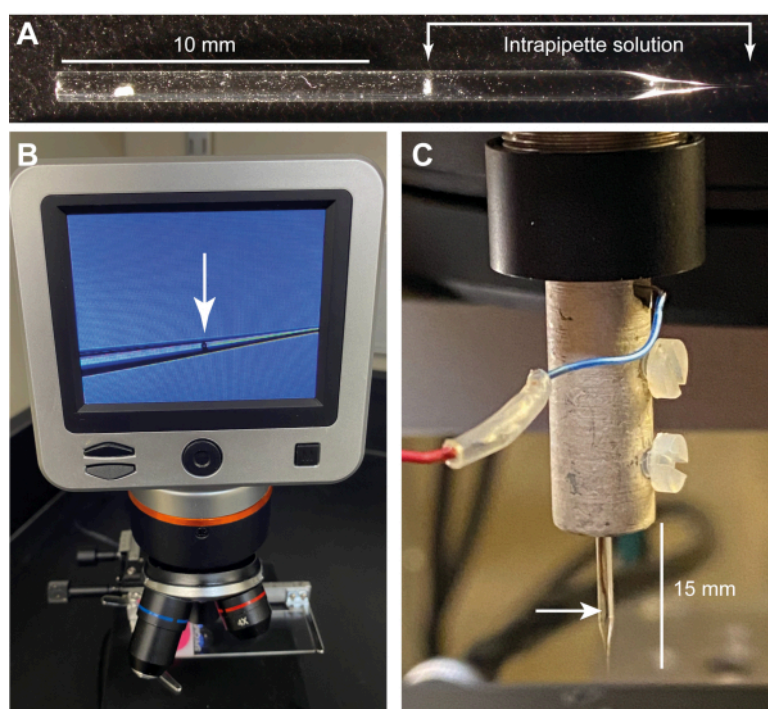


Figure 2: Nanopipette fabrication and filling. (A) An approximately 2 cm-long nanopipette filled with the intrapipette solution (HBSS). (B) An image of the bubble (arrow) that is typically formed after filling the pipette. The bubble usually moves away within few minutes of microscope illumination (an LCD digital microscope at 10x). (C) A nanopipette mounted into the SICM head. The arrow points to the AgCl electrode inside the pipette. Notice that the pipette holder is silver painted and grounded to minimize radiative electrical pickup from the Z piezo actuator. [Please click here to view a larger version of this figure.](#)

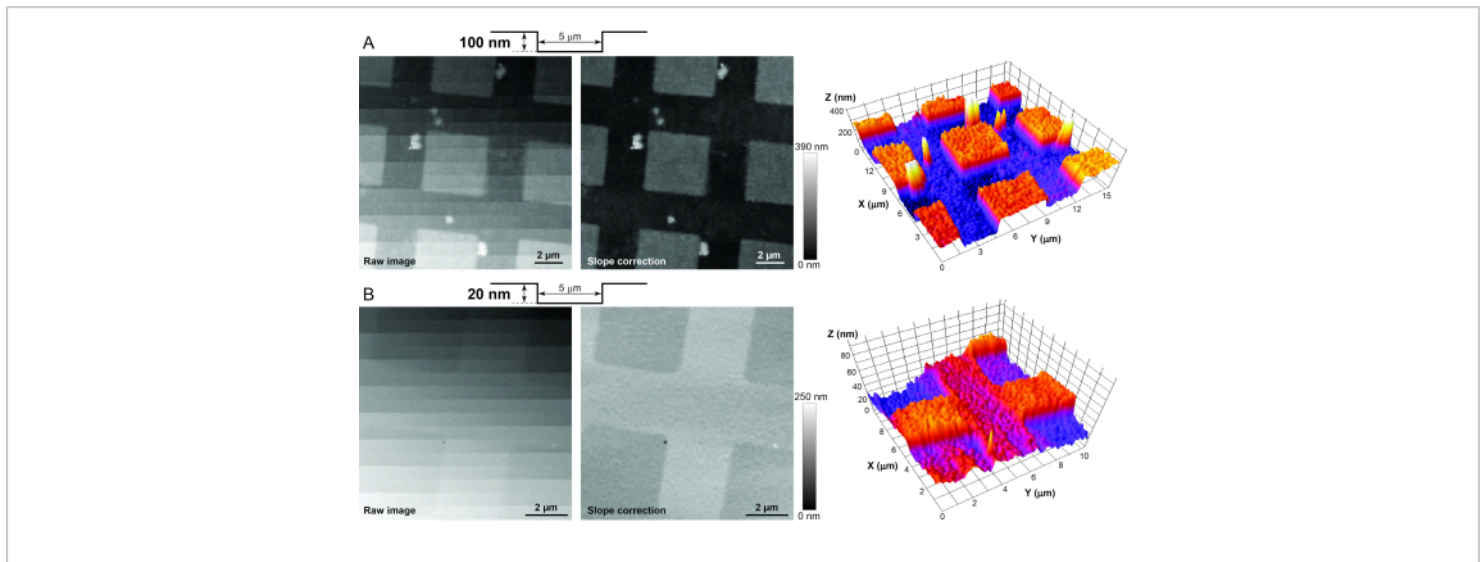


Figure 3: Imaging of AFM calibration standards to determine adequate stability, vibration isolation, and electrical noise in the system. (A) Raw (left), post-processed (middle), and 3D (right) images of the HS-100MG calibration standard. The surface profile of the standard is shown schematically at the top. Since the standard is never aligned perfectly perpendicular to the nanopipette, the post-processing slope correction is needed to reveal small vertical features of the sample. (B) Similar raw (left), post-processed (middle), and 3D (right) images of the HS-20MG calibration standard that has smaller, 20-nm deep indentations. Note that greyscale of a pixel in an HPICM image indicates the height of the sample at that point. [Please click here to view a larger version of this figure.](#)

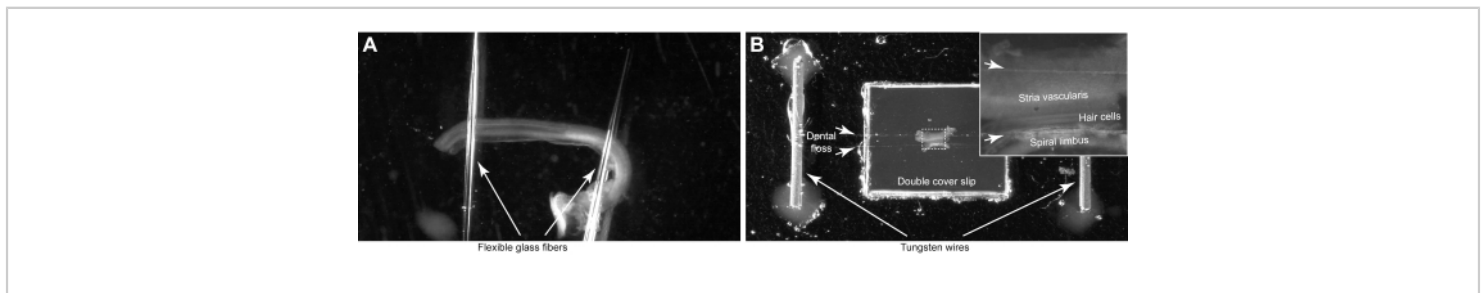


Figure 4: Mounting of the organ of Corti explant. (A) The explant is held by two glass pipettes that are glued to the glass-bottom Petri dish. (B) The explant is secured by two dental floss strands (arrows) in a custom-made imaging chamber. Inset shows magnified image of the organ of Corti. [Please click here to view a larger version of this figure.](#)

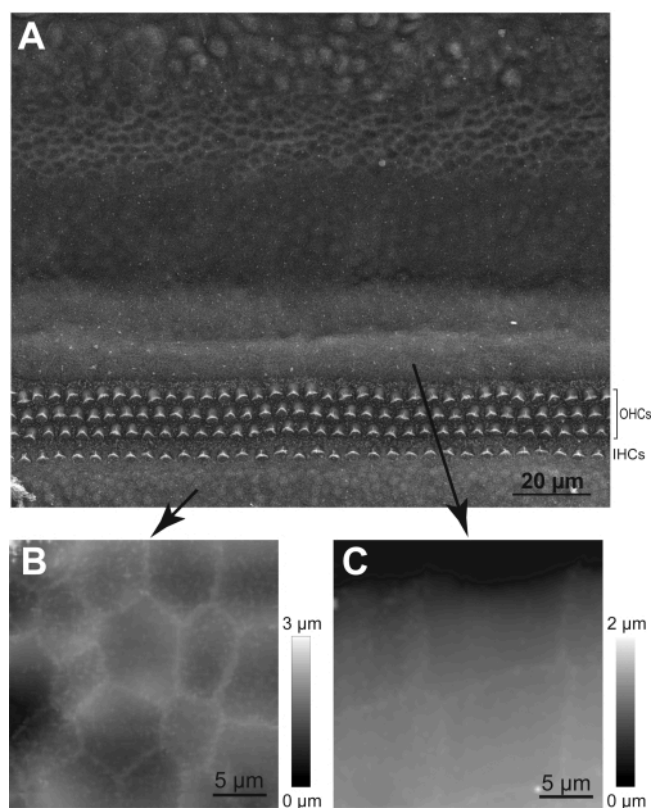


Figure 5: Navigation of the HPICM probe to the hair cell region. (A) SEM image of the cochlear explant showing rows of inner (IHCs) and outer (OHCs) hair cells and distinct types of supporting cells. (B) Representative HPICM image of the cells in Kolliker's organ. (C) An HPICM image of the Hensen's cells. Note that these two types of supporting cells have very distinct shapes, which helps determining whether the HPICM probe landed to an area that is radial or peripheral to the hair cells. [Please click here to view a larger version of this figure.](#)

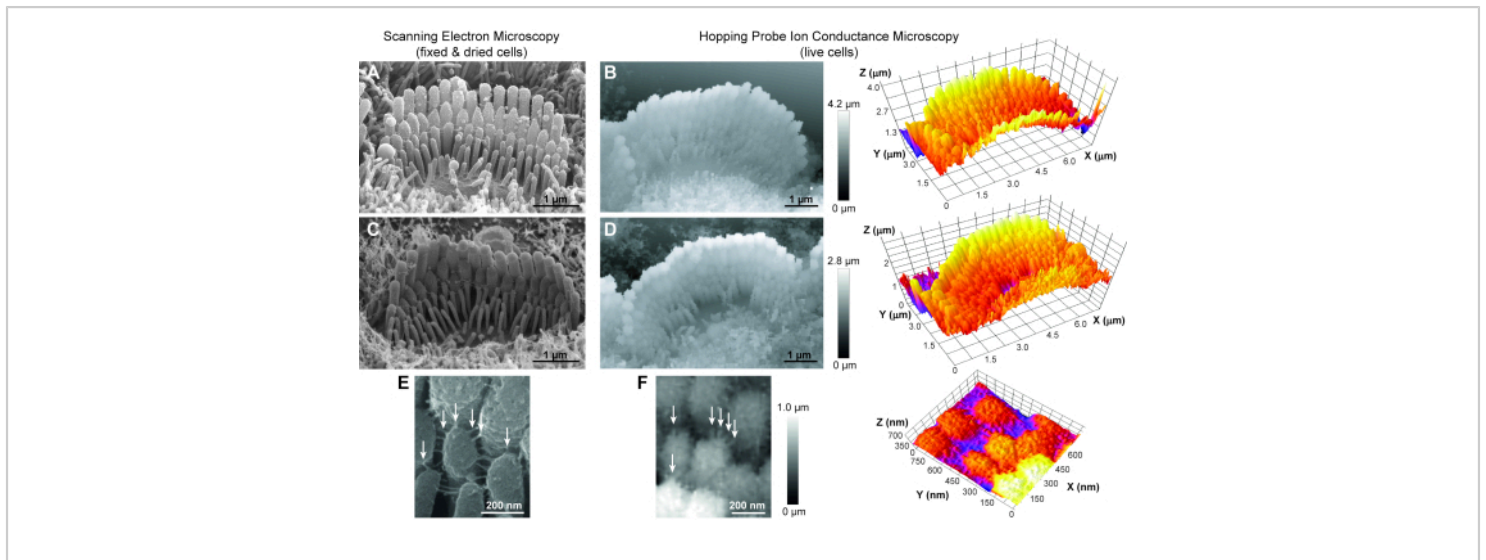


Figure 6: Comparison between scanning electron microscopy (SEM) and hopping probe ion conductance microscopy (HPICM) imaging of stereocilia bundles in young postnatal rodent inner hair cells. (A,C) SEM images provide sub-nanometer resolution of the surface details but in the cells that are fixed and shrunk due to critical point drying. In addition, SEM images do not allow 3D analysis. (B,D) HPICM images (left) have a worse resolution (~5-10 nm) but they are obtained in live cells, allow time lapse imaging, and carry information on exact heights, which allows 3D reconstruction and measurements (right). (E,F) Extracellular links between stereocilia are evident in both SEM (E) and HPICM (F) images (arrows). Cell ages: A, postnatal day 5 (P5) mouse; B, P6 rat; C, P8 mouse; D, P5 rat; E, P7 mouse; and F, P5 rat. In all HPICM images, greyscale of a pixel indicates the height of the sample at that point. [Please click here to view a larger version of this figure.](#)

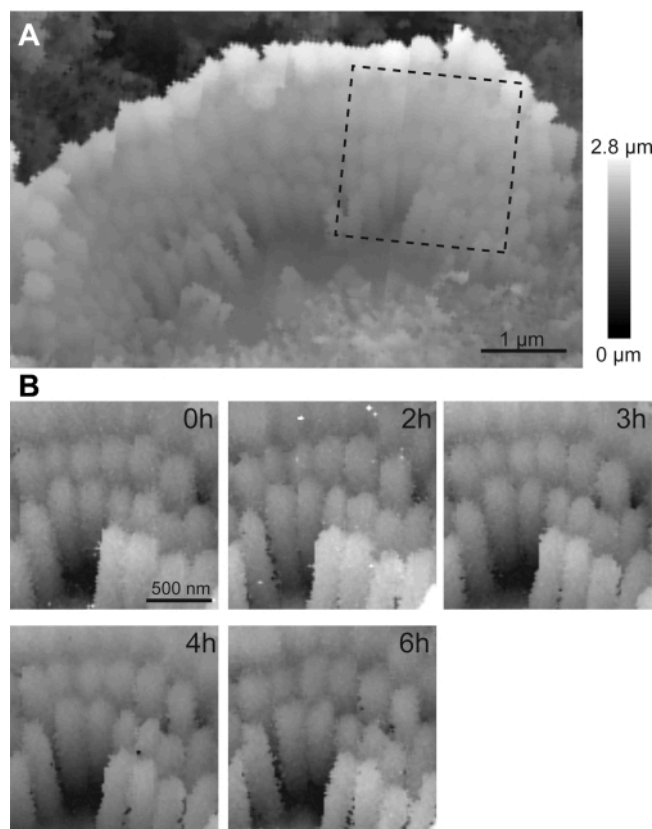


Figure 7: Continuous time lapse HPICM imaging of stereocilia bundle. (A) An overview of an inner hair cell bundle from P5 rat showing distinct shorter row stereocilia. (B) Time lapse imaging of the region of interest indicated in (A) throughout six hours. Note that, in contrast to a typical patch clamp experiment, the hair cells show no signs of deterioration for several hours in vitro. This is due to careful dissection and the absence of any mechanical disturbances to the cell. [Please click here to view a larger version of this figure.](#)

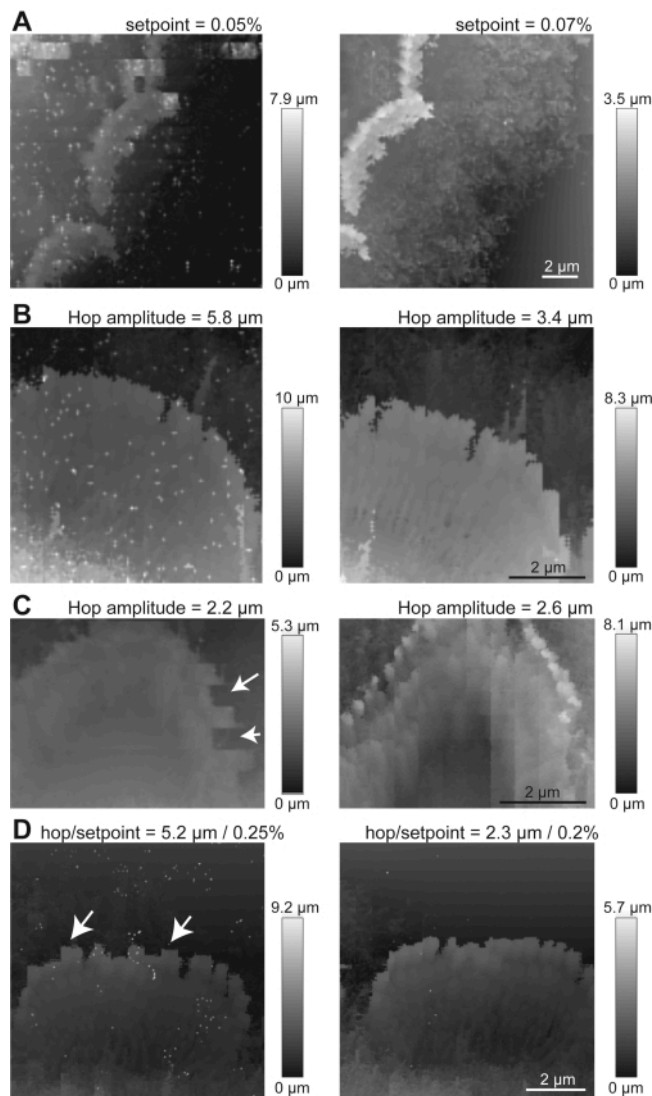


Figure 8: Common artefacts while imaging with HPICM. (A) Effect of a too low setpoint. Low-resolution HPICM images of the same live inner hair cell bundles in P3 mice acquired with setpoint 0.05% (left) and 0.07% (right). Notice a white dot noise that disappears with higher setpoint. (B) Effect of a too high hop amplitude. White dot noise also appears in an HPICM image of a P7 rat inner hair cell bundle obtained with a large hop amplitude of 5.8 μm (left). This noise disappears when the same bundle is imaged with the hop amplitude of 3.4 μm (right) due to the decrease of vibrations in the system. (C) Too low hop amplitude results in colliding of the HPICM probe to the stereocilia and dragging them (arrows on the left panel). Increasing the hop amplitude just enough to “climb over” stereocilia eliminates this artefact (right) but may also increase imaging time, resulting in a noticeable drift (vertical lines in the right panel). Stereocilia bundle of a live outer hair cell from P7 rat. (D) Too high setpoint causes a squared shape of stereocilia tips (arrows) in an HPICM image (left), again due to colliding of the nanopipette to the stereocilia. Decreasing setpoint (with simultaneous decrease of the hope amplitude to eliminate

white noise) improves the imaging (right). Stereocilia bundle of a live inner hair cell from P6 rat). [Please click here to view a larger version of this figure.](#)

Resolution	Image area (µm)	Lateral Resolution (nm)	Time per image (minutes)
Low	20×20	≥300	≤20
Low	10×10	≥156	≤15
Low	5×5	≥75	≤4
High	20×20	≤200	≤20
High	10×10	≤110	≤15
High	5×5	≤55	≤4

Table 1: Typical times of HPICM imaging depending on the size of imaging area and the scanning resolution.

Discussion

To obtain successful HPICM images, users need to establish a low noise and low vibration system and manufacture appropriate pipettes. We strongly recommend the use of AFM calibration standards to test the stability of the system before attempting to perform any live cell imaging. Once the resolution of the system is tested, users can consider imaging fixed organ of Corti samples to get familiar with the imaging settings before attempting any live cell imaging.

The optimal setpoint for imaging varies between different pipettes, depending on the individual shape of their tips (that is unknown until examined by electron microscopy) and on the amount of dirt attached to the tip, which is also unpredictable. Nanopipettes with an optimal setpoint higher than 7% should be discarded.

During imaging of live cells, the amount of dust and debris in the extracellular solution increases over time. All these particles can end up at the tip of the pipette, causing a reduction in the current and making it impossible to continue

scanning the tissue - the image will turn completely white since the feedback will "think" that the nanopipette is always in the vicinity of the sample. If this happens, it is recommended to retract the pipette in Z-axis from that area of the tissue. This retraction could clear the "dirtiness". If the pipette is still dirty, it is necessary to change the pipette and move to a different area of the sample. Then, the user can continue to scan the tissue.

As of today, the most essential limitation of the HPICM is the amount of time required to take an image at high resolution while working with samples with complex topography. Depending on the resolution desired, images can take up to half an hour or more. In images acquired for longer than fifteen minutes, the drift may become evident and specific structures may be shifted and harder to distinguish. This is happening because the living cells are constantly moving or changing their shape over time. To visualize molecular events and changes in cells' structures over time, further developments are needed to optimize the temporal resolution of the HPICM¹¹.

The noise of the nanopipette current represents another limitation because it sets the minimal practically achievable setpoint. The current generated by the nanopipette in the solution attenuates quickly (inverse proportional to the cubic distance from the pipette tip), thereby establishing a “sensing volume”, beyond which the nanopipette cannot “sense” the surface. We have previously developed a model of this phenomenon and showed that the lateral resolution of the SICM probe is determined by the cross-section of this “sensing volume” with the cell surface, which could be extremely small at low setpoints²⁵. This is particularly important for imaging hair cell tip links that have a diameter of ~5 nm^{12,33}. On the first glance, the pipettes with smaller inner diameter would result in better resolution of HPICM imaging. This is indeed true for relatively large pipettes (>50 nm). However, decreasing the inner diameter of the nanopipette below ~50 nm results in unproportionally large increase of the pipette noise and, hence, the loss of resolution at low setpoints that are essential for imaging stereocilia bundles. As of today, we do not know how to solve this problem and we are working on finding the proper solution.

In summary, this paper presents a detailed protocol for the visualization of stereocilia bundles in live mammalian auditory hair cells with HPICM. The biggest advantages of the HPICM are: i) its ability to visualize label-free nanoscale structures at the surface of living cells without touching them; and ii) to probe the function of these structures with patch clamp recordings and/or local nanoscale delivery of mechanical or chemical stimuli. To the best of our knowledge, these advantages are unique to HPICM. Of course, there are some disadvantages. First, due to limitations on the height of the structures to be imaged, HPICM may not be suitable for imaging extremely tall structures, such as stereocilia bundles of the vestibular hair cells in the mammalian ampullae.

Second, HPICM is still developing and further improvements in the speed and resolution of imaging are needed. However, the physical principles of HPICM and our own experience suggest that it is possible. We do believe that HPICM will provide unique data on the function of individual protein complexes at the stereocilia surface.

Disclosures

The authors have no competing interests.

Acknowledgments

We thank Prof. Yuri Korchev (Imperial College, UK) for the long-term support and advice throughout all stages of the project. We also thank Drs. Pavel Novak and Andrew Shevchuk (Imperial College, UK) as well as Oleg Belov (National Research Centre for Audiology, Russia) for their help with software development. The study was supported by NIDCD/NIH (R01 DC008861 and R01 DC014658 to G.I.F.).

References

1. Beurg, M., Fettiplace, R., Nam, J. H., Ricci, A. J. Localization of inner hair cell mechanotransducer channels using high-speed calcium imaging. *Nature Neuroscience*. **12** (5), 553-558 (2009).
2. Effertz, T., Becker, L., Peng, A. W., Ricci, A. J. Phosphoinositol-4,5-bisphosphate regulates auditory hair-cell mechanotransduction-channel pore properties and fast adaptation. *The Journal of Neuroscience: the Official Journal of the Society for Neuroscience*. **37** (48), 11632-11646 (2017).
3. Peng, A. W., Gnanasambandam, R., Sachs, F., Ricci, A. J. Adaptation independent modulation of auditory hair cell mechanotransduction channel open probability implicates a role for the lipid bilayer. *The Journal of*

- Neuroscience: the Official Journal of the Society for Neuroscience*. **36** (10), 2945-2956 (2016).
4. Engström, H., Engström, B. Structure of the hairs on cochlear sensory cells. *Hearing research*. **1** (1), 49-66 (1978).
5. Conchello, J.-A., Lichtman, J. W. Optical sectioning microscopy. *Nature Methods*. **2** (12), 920-931 (2005).
6. Sigal, Y. M., Zhou, R., Zhuang, X. Visualizing and discovering cellular structures with super-resolution microscopy. *Science*. **361** (6405), 880-887 (2018).
7. Wäldchen, S., Lehmann, J., Klein, T., van de Linde, S., Sauer, M. Light-induced cell damage in live-cell super-resolution microscopy. *Scientific Reports*. **5** , 15348 (2015).
8. Pickles, J. O., Comis, S. D., Osborne, M. P. Cross-links between stereocilia in the guinea pig organ of Corti, and their possible relation to sensory transduction. *Hearing Research*. **15** (2), 103-112 (1984).
9. Furness, D. N., Hackney, C. M. Cross-links between stereocilia in the guinea pig cochlea. *Hearing Research*. **18** (2), 177-188 (1985).
10. Jacobs, R. A., Hudspeth, A. J. Ultrastructural correlates of mechano-electrical transduction in hair cells of the bullfrog's internal ear. *Cold Spring Harbor Symposia on Quantitative Biology*. **55** , 547-561 (1990).
11. Goodyear, R. J., Marcotti, W., Kros, C. J., Richardson, G. P. Development and properties of stereociliary link types in hair cells of the mouse cochlea. *The Journal of Comparative Neurology*. **485** (1), 75-85 (2005).
12. Kachar, B., Parakkal, M., Kurc, M., Zhao, Y., Gillespie, P. G. High-resolution structure of hair-cell tip links. *Proceedings of the National Academy of Sciences of the United States of America*. **97** (24), 13336-13341 (2000).
13. Vélez-Ortega, A.C., Freeman, M. J., Indzhykulian, A. A., Grossheim, J. M., Frolenkov, G. I. Mechanotransduction current is essential for stability of the transducing stereocilia in mammalian auditory hair cells. *eLife*. **6**, 1-22 (2017).
14. Ivanchenko, M. V et al. Serial scanning electron microscopy of anti-PKHD1L1 immuno-gold labeled mouse hair cell stereocilia bundles. *Scientific Data*. **7** (1), 182 (2020).
15. Hadi, S., Alexander, A. J., Vélez-Ortega, A. C., Frolenkov, G. I. Myosin-XVa controls both staircase architecture and diameter gradation of stereocilia rows in the auditory hair cell bundles. *Journal of the Association for Research in Otolaryngology: JARO*. **21** (2), 121-135 (2020).
16. Metlagel, Z. et al. Electron cryo-tomography of vestibular hair-cell stereocilia. *Journal of Structural Biology*. **206** (2), 149-155 (2019).
17. Langer, M. G. et al. Mechanical stimulation of individual stereocilia of living cochlear hair cells by atomic force microscopy. *Ultramicroscopy*. **82** (1-4), 269—278 (2000).
18. Dufrêne, Y .F. Towards nanomicrobiology using atomic force microscopy. *Nature Reviews Microbiology*. **6** (9), 674-680 (2008).
19. Putman, C. A., van der Werf, K. O., de Grooth, B. G., van Hulst, N. F., Greve, J. Viscoelasticity of living cells allows high resolution imaging by tapping mode atomic force microscopy. *Biophysical journal*. **67** (4), 1749-1753 (1994).

20. Gavara, N., Chadwick, R. S. Noncontact microrheology at acoustic frequencies using frequency-modulated atomic force microscopy. *Nature Methods*. **7** (8), 650-654 (2010).
21. Cartagena-Rivera, A. X., Van Itallie, C. M., Anderson, J. M., Chadwick, R. S. Apical surface supracellular mechanical properties in polarized epithelium using noninvasive acoustic force spectroscopy. *Nature Communications*. **8** (1), 1030 (2017).
22. Katsuno, T. et al. TRIOBP-5 sculpts stereocilia rootlets and stiffens supporting cells enabling hearing. *JCI Insight*. **4** (12) (2019).
23. Hansma, P. K., Drake, B., Marti, O., Gould, S. A., Prater, C. B. The scanning ion-conductance microscope. *Science*. **243** (4891), 641-643 (1989).
24. Korchev, Y. E. et al. Specialized scanning ion-conductance microscope for imaging of living cells. *Journal of Microscopy*. **188** (Pt 1), 17-23 (1997).
25. Shevchuk, A. I. et al. Imaging proteins in membranes of living cells by high-resolution scanning ion conductance microscopy. *Angewandte Chemie (International ed in English)*. **45** (14), 2212-2216 (2006).
26. Novak, P. et al. Nanoscale live-cell imaging using hopping probe ion conductance microscopy. *Nature Methods*. **6** (4), 279-281 (2009).
27. Vélez-Ortega, A. C., Frolenkov, G. I. Visualization of live cochlear stereocilia at a nanoscale resolution using hopping probe ion conductance microscopy. *Methods in Molecular Biology*. **1427**, 203-221 (2016).
28. Gu, Y. et al. High-resolution scanning patch-clamp: new insights into cell function. *FASEB Journal: Official Publication of the Federation of American Societies for Experimental Biology*. **16** (7), 748-750 (2002).
29. Frolenkov, G. I. et al. Single-channel recordings from the apical surface of outer hair cells with a scanning ion conductance probe. *Association for Research in Otolaryngology. Abs.* 444, (2004).
30. Sánchez, D. et al. Noncontact measurement of the local mechanical properties of living cells using pressure applied via a pipette. *Biophysical Journal*. **95** (6), 3017-3027 (2008).
31. Korchev, Y. E., Negulyaev, Y. A., Edwards, C. R., Vodyanoy, I., Lab, M. J. Functional localization of single active ion channels on the surface of a living cell. *Nature Cell Biology*. **2** (9), 616-619 (2000).
32. Shevchuk, A. et al. Angular approach scanning ion conductance microscopy. *Biophysical Journal*. **110** (10), 2252-2265 (2016).
33. Furness, D. N., Katori, Y., Nirmal Kumar, B., Hackney, C. M. The dimensions and structural attachments of tip links in mammalian cochlear hair cells and the effects of exposure to different levels of extracellular calcium. *Neuroscience*. **154** (1), 10-21 (2008).